

Experimental evidence for α production following neutron transfer in the $^{13}\text{C} + ^{93}\text{Nb}$ system

H. Kumawat ^{1,2,*} V. V. Parkar ^{1,2} T. N. Nag,^{2,3} R. Tripathi,^{2,3} V. Jha,^{1,2} S. Santra,^{1,2} and S. Kailas ^{1,4}

¹Nuclear Physics Division, Bhabha Atomic Research Centre, Mumbai 400085, India

²Homi Bhabha National Institute, Anushaktinagar, Mumbai 400094, India

³Radiochemistry Division, Bhabha Atomic Research Centre, Mumbai 400085, India

⁴UM-DAE Centre for Excellence in Basic Science, Mumbai 400098, India



(Received 29 June 2021; revised 15 September 2021; accepted 4 February 2022; published 18 February 2022)

Spectra of α particles were measured for $^{12,13}\text{C} + ^{93}\text{Nb}$ systems at several angles for a bombarding energy of 65 MeV to investigate various reaction mechanisms like direct break up and cluster transfer responsible for α production. The α spectra were analyzed in detail to determine the effect of $1n$ transfer on an α -production cross section in particular. After accounting for contributions from direct breakup and Be transfer, there is a clear signature of the α particles produced through the break-up process following neutron transfer in the case of a ^{13}C induced reaction. This is an interesting result being reported for the strongly bound projectile.

DOI: [10.1103/PhysRevC.105.024611](https://doi.org/10.1103/PhysRevC.105.024611)

I. INTRODUCTION

The occurrence of clusters is well known in macroscopic and microscopic matter, ranging from astrophysics to nuclear physics [1]. The α -particle clustering influences their emission from heavy nuclei [2–9]. In heavy ion reactions, projectile structure has an influence on the yield of projectile-like fragments (PLF) [10]. Yields of PLFs with $Z = 6$ and 8 were observed to be higher than odd Z PLFs in the ^{20}Ne -induced reaction on several targets [11,12]. Measurement of incomplete fusion cross section showed a higher cross section for the ^{12}C projectile compared to the ^{13}C projectile [13–15] which was attributed to α -particle Q values and the structure of the ^{12}C projectile. In addition to the projectile structure, ICF cross sections depend on entrance channel mass asymmetry, angular momentum, target deformation, etc. [16,17]. Similarly, the observation of a large α -production cross section is an important feature of heavy ion induced reactions at Coulomb barrier energies [18]. In the case of weakly bound stable projectiles like $^6,7\text{Li}$ and ^9Be , the inclusive α -cross sections form a substantial portion of the corresponding reaction cross sections. However, in the case of strongly bound projectiles like ^{12}C , ^{14}N , and ^{16}O , the α -cross sections are significant but are not more than 10–20 % of the corresponding reaction cross sections [19,20]. In view of its importance, a large number of experiments and theoretical investigations have been carried out to understand the mechanisms for α production in heavy ion reactions. In the case of weakly bound projectiles, break up and capture/transfer are the dominant mechanisms responsible for α emission. It has been shown that a significant amount of α particles is also produced following particle transfer from the projectile to target (and particle transfer from

target to projectile) [21]. In the case of strongly bound projectiles, direct break up and cluster transfer have been shown to be responsible for α production [6,22]. The α spectra could be fully understood by invoking the above two mechanisms for the ^{12}C projectile [23,24].

The direct α -production cross sections show an interesting correlation with the α -binding energies of the projectiles [25,26]. It turns out that in the case of projectiles with mass numbers lying between 6 and 20, the α -binding energies of the projectiles are the smallest when compared to proton and neutron binding energies. This being the case, the observed correlation between α -cross sections and α -binding energies can be understood. However, in the case of ^{13}C , the neutron binding energy is 4.95 MeV which is less than its α -binding energy of 10.65 MeV. Hence, the neutron transfer from ^{13}C is expected to be significant and it is conceivable that in the case of ^{13}C induced reactions, α particles can arise not only from direct break up and cluster transfer processes (like ^9Be transfer to target), but also from break up following neutron transfer, ^9Be breakup following α transfer, and ^8Be breakup following ^5He transfer. It will be interesting to look for an experimental evidence for these processes and disentangle their relative contributions. In the literature, ^{13}C induced reaction data at Coulomb barrier energies are rather scarce. There are only a few papers which have reported α -emission cross sections in ^{13}C induced reactions [27]. However, the mechanisms for α emission have not been investigated.

With a view to understand the various mechanisms responsible for α emission in general and α emission following neutron transfer, in particular, detailed measurements have been carried out for α particles emitted in the ^{13}C induced reactions on ^{93}Nb . While the neutron binding energy is smaller than α -binding energy in the case of ^{13}C the neutron binding energy is very large when compared to α -binding energy for ^{12}C . Because of the large negative Q value of the ^{12}C induced neutron transfer reaction, we expect the α emission following

*harphool@barc.gov.in

neutron transfer from the projectile to be much less in this case when compared to that from the ^{13}C induced reaction. Keeping this in mind, in addition to ^{13}C , α particles emitted in the ^{12}C induced reactions on ^{93}Nb have also been measured. As one neutron transfer cross section is expected to be significant for ^{13}C , the cross section also has been measured for a comparative study with the α -emission channel. A detailed analysis of the α - and neutron transfer data has been carried out. The α -particles spectra from ^{12}C and ^{13}C have been compared and, in the case of ^{13}C , the α particles from breakup following neutron transfer have been clearly identified.

II. EXPERIMENTAL DETAILS

Details of the experimental setup are given in Ref. [28] and a brief summary is given. The experiment was carried out at BARC-TIFR Pelletron LINAC facility, Mumbai, India. A self-supporting ^{93}Nb target of thickness $\approx 400 \mu\text{g}/\text{cm}^2$ was bombarded with 65 MeV $^{12,13}\text{C}$ beams in a 1.5 m diameter scattering chamber. Ten silicon surface barrier detector (ΔE - E) telescopes were used to detect the outgoing projectile-like fragments (PLF) with $Z = 3-7$ along with lighter fragments like ^4He . The angular distributions of PLFs and ^4He were measured in the angular range of $20^\circ - 105^\circ$. The PLF distributions are reported in Ref. [28] except for the α production. Total PLF (for fragments heavier than the α particle) production cross sections add up to ≈ 30 mb and ≈ 40 mb for $^{13}\text{C} + ^{93}\text{Nb}$ and $^{12}\text{C} + ^{93}\text{Nb}$ systems, respectively. In addition, ^{13}C has a significant part of $1n$ -transfer cross-section producing ^{12}C as PLF which was excluded in the above-mentioned PLF cross-section values. In the present work, α spectra and their angular distributions are discussed in detail.

III. EXPERIMENTAL ENERGY AND ANGULAR DISTRIBUTIONS

The elastic peaks at different angles were used for the energy calibration and α -energy spectra were obtained. The α spectra in the angular range $\theta_{\text{lab}} = 25-70^\circ$ is shown in Fig. 1 [(a)–(d) for ^{13}C and (e)–(h) for ^{12}C projectile]. Here, compound nuclear reaction (denoted as CF) and noncompound nuclear reaction or direct (denoted as NCF) contributions are shown separately. The measured α spectra contain contributions from both direct and compound nuclear reaction components. The direct part is composed of α particles originating from direct breakup of the projectile as well as α particles emitted along with transfer of $^9,8\text{Be}$ to the target through the reactions $^{93}\text{Nb}(^{13}\text{C}, ^4\text{He})^{102}\text{Rh}$ and $^{93}\text{Nb}(^{12}\text{C}, ^4\text{He})^{101}\text{Rh}$. There will be additional contributions due to the reactions of the type $^{93}\text{Nb}(^{13}\text{C}, ^9\text{Be})^{97}\text{Tc}$ and $^{93}\text{Nb}(^{12}\text{C}, ^8\text{Be})^{97}\text{Tc}$ followed by a break up of ^9Be and ^8Be leading to α production. The α -particle energy distributions from evaporation are of typical Maxwellian shapes whereas those from breakup and transfer reactions are of Gaussian in nature [29–31]. The contribution of the direct part falls off exponentially with angle. The angular distribution of one neutron transfer channel for

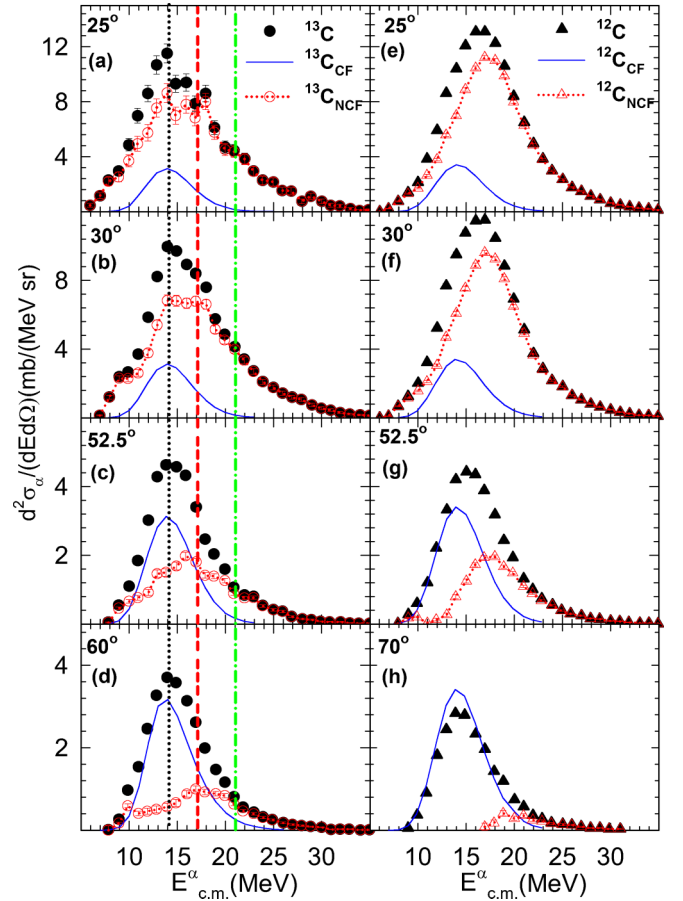


FIG. 1. α -particle energy spectra for $^{12,13}\text{C} + ^{93}\text{Nb}$ system at $\theta_{\text{lab}} = 25-70^\circ$ at 65 MeV. Here, left (a)–(d) and right (e)–(h) side plots are for ^{13}C and ^{12}C projectiles, respectively. Compound nuclear contribution (CF) is depicted by continuous lines. Total (compound + direct), direct (NCF) cross sections are denoted by filled and empty circles (^{13}C) and triangles (^{12}C), respectively. Dotted, dashed, and dash-dotted lines for ^{13}C are at 14.3, 17.3, and 21.1 MeV, respectively, corresponding to most probable energies for breakup (BUP), transfer-breakup (TR-BUP), and transfer (TR) channels.

the $^{13}\text{C} + ^{93}\text{Nb}$ system was also analyzed and the contributions from the discrete and continuum transfer modes were separated.

The experimental energy integrated differential cross section was obtained using the equation from Ref. [32] as follows:

$$\frac{d\sigma_\alpha}{d\Omega} = \frac{Y_\alpha}{Y_{el}} \times \frac{d\sigma_{el}}{d\Omega}. \quad (1)$$

Here, $d\sigma_{el}/d\Omega$ is the elastic scattering cross section, published earlier [28], Y_α and Y_{el} are α -particle and elastic counts, respectively.

The statistical model calculations were performed using PACE2 [33]. The Ignatyuk prescription of level density (with $\tilde{a} = A/7\text{MeV}^{-1}$, A = mass number) was used. The model parameters were fixed to reproduce the α -cross section for nearby systems $^{12}\text{C} + ^{51}\text{V}$ [34] and $^{12}\text{C} + ^{115}\text{In}$ [35] at backward angles where a contribution from compound nuclear

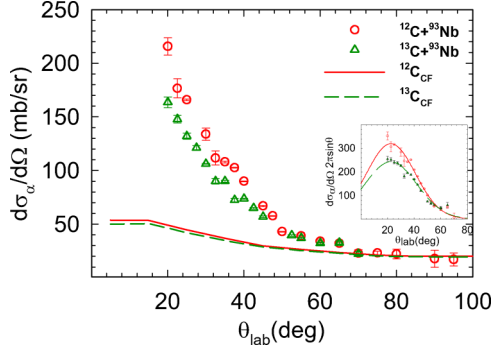


FIG. 2. Energy integrated angular distribution are represented by circles and triangles for ^{12}C , ^{13}C , respectively. Compound nuclear contribution (CF) is depicted by solid and dashed lines for ^{12}C , ^{13}C , respectively. Gaussian fits of direct (total-compound) α -production cross sections for $^{12,13}\text{C}$ are shown in the inset.

reaction is dominant. The present analysis is done with the same set of parameters.

The angular distributions of α -particle production cross sections are shown in Fig. 2. It is evident that the back angle cross section has contribution from the compound reaction mechanism only and the magnitude of direct contribution decreases exponentially with angle. The compound nuclear reaction cross section was subtracted from the total α -cross section to obtain the contribution from breakup/transfer reactions. The total α -cross section can be obtained by extrapolating to forward angles either by an exponential function to the $d\sigma/d\Omega$ or a Gaussian fit to $2\pi\sin\theta \times d\sigma/d\Omega$. Both methods give similar results within quoted error bars. The direct/noncompound angular distributions which were fitted assuming a Gaussian shape of $(2\pi\sin\theta \times d\sigma/d\Omega)$ distribution, are given in inset of Fig. 2. From this fit, the angle and energy integrated direct α -cross section for ^{12}C and ^{13}C are determined as 226 ± 25 mb and 187 ± 40 mb, respectively. The errors in the cross sections were estimated from the errors in the fitted parameters.

The ratio of α -production cross sections for ^{12}C and ^{13}C projectiles is 1.2 ± 0.3 which is close to 1.3 ± 0.27 reported for ^{48}Ti [27] (in the present measurement, the measured angular range contributes 80% of the direct cross section and the ratio of direct α -production cross sections in this angular range is 1.2 ± 0.18).

IV. KINEMATIC DISENTANGLEMENT OF α -PARTICLE ENERGY SPECTRA

Detailed analysis of the α -energy spectra was carried out to understand the mechanisms responsible for α production. The direct α -energy spectra, as shown in Fig. 1, from ^{13}C are much broader than the ones from ^{12}C (FWHM values for ^{13}C are at least 25% higher than that for ^{12}C). The prominent peak in the case of ^{12}C is around 18 MeV. The breakup α energy is estimated to be around 16.7 MeV for the ^{12}C projectile. A leading order expression proposed by Schiffer for Q_{opt} was used which is given as $E_{c.m.} (Z_3 Z_4 / Z_1 Z_2 - 1)$ [36], where Z_1 , Z_2 , Z_3 , Z_4 are the atomic numbers of the projectile, target,

TABLE I. Kinematic parameters for α and $^{8,9}\text{Be}$ transfer channels for the $^{12,13}\text{C} + ^{93}\text{Nb}$ system at $E_{\text{lab}} = 65$ MeV ($E_{c.m.} = 57.6$ MeV and 57 MeV for $^{12,13}\text{C}$, respectively). Q_{gg} represent transfer to ground state, the expected optimum Q value (Q_{opt}) calculated at leading order according to Refs. [36,38], centroid energy of the direct α for the respective channels in the c.m. system ($\bar{E}_\alpha = E_{c.m.} + Q_{gg} + Q_{\text{opt}}$). ^8Be is assumed to be broken having 92 keV binding energy by releasing two α particles. The energies of breakup constituents are calculated as per mass ratio.

Proj.		α trans. (MeV)	^8Be trans. (MeV)	3α breakup (MeV)
^{12}C	Q_{gg}	-4.9	-2.2	-7.27
	Q_{opt}	-17.3	-36.5	0.0
	\bar{E}_α	17.7	18.8	16.7
		$1n$ trans. (MeV)	^9Be trans. (MeV)	$\alpha + ^9\text{Be}$ breakup (MeV)
^{13}C	Q_{gg}	2.3	0.3	-10.6
	Q_{opt}	0.0	-36.2	0.0
	\bar{E}_α	17.3	21.1	14.3

ejectile, and residual nucleus. The experimental PLF kinetic energy spectra [28] were converted to the c.m. system and Q_{opt} values were deduced from these data. The experimental Q_{opt} values agreed very well with the Q_{opt} values (within experimental uncertainties) obtained using the Schiffer expression. Having validated the use of Schiffer's expression for Q_{opt} , we used the same for α and Be transfers in the present work. There is also another expression for Q_{opt} from Mermaz [37] and values obtained by the formulation are also close to the experimental values for the channels considered here. The α particle coming along with the transfer of ^8Be to ^{93}Nb is estimated to be centered around 18.8 MeV, taking the Q_{opt} to be around -36.5 MeV. Table I gives kinematic parameters and centroid energies for different reaction channels. The centroid energy of the direct α for the respective channels in the c.m. system is calculated as $(E_\alpha = E_{c.m.} + Q_{gg} + Q_{\text{opt}})$. Q_{opt} is taken as zero for breakup process and the available excitation energy is divided as per mass proportion into the fragments. As the α peak in the case of ^{12}C is centered around 18 MeV, and there is no clear indication of a peak at energies below 16 MeV, perhaps it can be concluded that the α particles in this case are mainly from the break up of the projectile and α particles emitted along with the transfer of ^8Be . There can also be the processes like the transfer of ^4He from ^{12}C to ^{93}Nb and subsequent break up of ^8Be . The α particles coming from this process is estimated to be centered around 17.7 MeV, taking the Q_{opt} to be around -17.3 MeV. (Here, the two α -particles energies were obtained by dividing the $E_{c.m.} + Q_{gg} + Q_{\text{opt}}$ value by two).

However, in the case of ^{13}C , the projectile break up α particles are expected to peak around 14.3 MeV and the one coming along with ^9Be transfer is estimated to be around 21.1 MeV. The α particle emitted from the break up of ^{12}C formed after the neutron transfer from ^{13}C is calculated to be around 17.3 MeV. In addition, there can be processes like α transfer, followed by break up of ^9Be in the case of ^{13}C induced reactions. The energies of α particles from this reaction

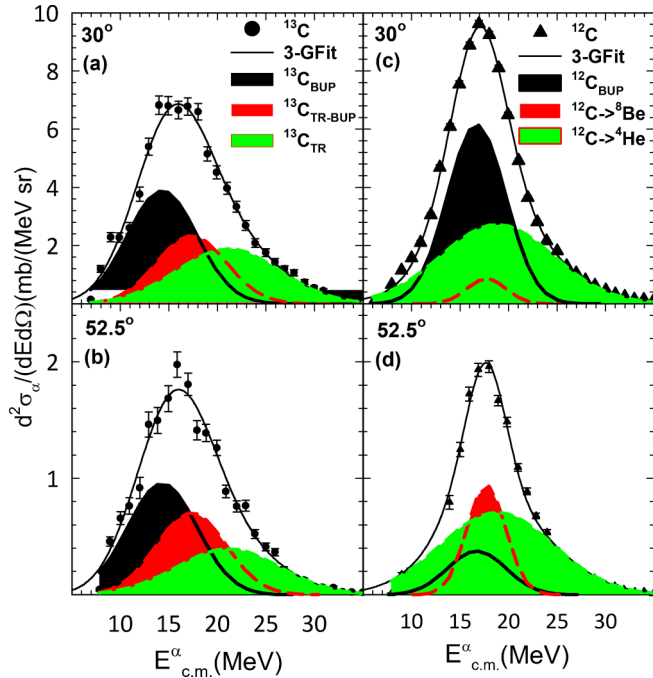


FIG. 3. Identifying the α source from breakup (BUP), ^9Be transfer (TR), and $1n$ transfer followed by breakup (TR-BUP) for ^{13}C by fitting Gaussian shapes at peak energies of 14.3, 17.3, 21.1 MeV are shown in the left panels (a,b) and peak energies at 16.7, 17.7, 18.8 MeV for ^{12}C projectile for BUP, α transfer, and ^8Be transfer, respectively, are shown in the right panels (c), (d).

will come close to the one from neutron transfer followed by break up of ^{12}C . It is found that experimental data for neutron transfer is nearly 100 mb whereas the cross section for α transfer leading to production of ^9Be is less than 5 mb [28]. In view of this, we may expect the contribution of α particles from ^9Be break up in the region of interest (17.3 MeV) may not be significant. Another mechanism which can contribute to α particles in this energy region is the (^{13}C , ^8Be) reaction (^5He transfer) followed by the break up of ^8Be . As discussed above, we expect α and ^5He transfer contributions to be not as significant as neutron transfer cross sections. Further, even from the structure point of view ^{13}C is more likely to be $^{12}\text{C}+n$ and $^9\text{Be} + ^4\text{He}$ configurations in terms of binding energies. The break up threshold for ^{13}C into $^8\text{Be} + ^5\text{He}$ is about 2.5 MeV larger than that for the $^9\text{Be} + ^4\text{He}$ process. The calculation performed using the GRAZING [39] heavy ion reaction code also gives a cross section less than 1 mb for these channels. The measured α -energy spectra at all angles (20° – 70°) were analyzed by fitting Gaussian shapes for the various processes leading to α emission while keeping the fixed centroid energies estimated for breakup (BUP), transfer (TR), and transfer followed breakup (TR-BUP) (as shown in Fig. 3 at a few angles). In order to fix widths, initial fittings were done at 4–5 angles by keeping it as a free parameter. These widths were varying within 10% at different angles thus the average values for each process were obtained for final fitting. In the case of ^{12}C , besides direct break up, α particles resulting from ^8Be transfer accompanied by α particle (transfer channel one)

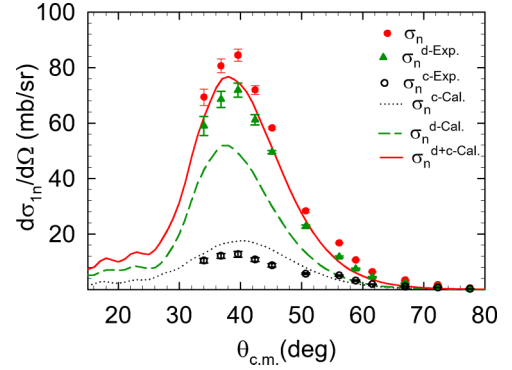


FIG. 4. Measured total, discrete, and continuum $1n$ -transfer cross section for $^{13}\text{C} + ^{93}\text{Nb}$ at 65 MeV are denoted by filled circles, triangles, and empty circles, respectively. The dotted and dashed lines show the estimated contribution for transfer to continuum and discrete states, respectively. The sum of both is represented by solid lines.

and ^4He transfer accompanied by ^8Be (transfer channel two) and its break up resulting into two α particles were also taken into account. In the case of ^{13}C , direct break up, ^9Be transfer accompanied by α -particle emission as well as neutron transfer followed by break up of ^{12}C leading to α particles have been considered. An estimate has been made for the relative contributions of the various processes contributing to α emission by the above-mentioned fitting procedure. Angular distributions for all processes similar to Fig. 2 were obtained to get the integral values for each process. In the case of ^{12}C , it is observed that the direct break up α particles are about 40%. It is estimated that the α particles accompanying ^8Be transfer is to be 50%. The α transfer with accompanying ^8Be and its breakup leading to α particles contribute about 10% of inclusive α particles produced in the reaction. In the case of ^{13}C , the direct break up α particles are 33% and the α particles accompanying ^9Be transfer is 43% of the inclusive α particles. In addition, it is observed that the α particles resulting from the process of one neutron transfer followed by the break up of ^{12}C , leads to α particles of the order of 24% of the total α particles. As we do not know the multiplicity values of α particles arising from direct break up and break up following $1n$ transfer, we cannot determine the α -cross sections for these processes. The estimation of direct breakup is affected by evaporation estimates as the coinciding α -particle peaks. The χ^2 values for single, double, and triple peak fittings were in the range of (3–15), (1.5–3), and (0.7–1.3), respectively. The errors in the integral values were estimated by varying the centroid values by 1 MeV around it (uncertainties in the Q_{opt} and energy calibration) which gives an estimate of around 15% in the relative fractions of integral values.

The angular distribution of the $1n$ transfer was obtained by the detection of the ^{12}C fragment following $1n$ transfer through the $^{93}\text{Nb}(^{13}\text{C}, ^{12}\text{C})^{94}\text{Nb}$ reaction. The ^{12}C band in the PLF spectra was measured from $Q = +2.28$ MeV ahead of ^{13}C elastic peak down to ≈ 20 MeV. The angular distribution of the $1n$ -transfer cross section measured for the $^{13}\text{C} + ^{93}\text{Nb}$ system is shown in Fig. 4. It shows the familiar bell shape with

TABLE II. Experimental cross sections for reaction (σ_R), noncompound α production ($\sigma_\alpha^{\text{NCF}}$), PLF (heavier than α) transfer (σ_{tr}^{PLF}), $1n$ -transfer total (σ_n^{tot}), $1n$ -transfer discrete ($\sigma_n^{d-\text{exp}}$), $1n$ -transfer continuum ($\sigma_n^{c-\text{exp}}$) and calculated $1n$ -transfer to discrete and continuum states ($\sigma_n^{d-\text{Cal.}}$, $\sigma_n^{c-\text{Cal.}}$) for the $^{12,13}\text{C} + ^{93}\text{Nb}$ system.

Proj.	σ_R (mb)	$\sigma_\alpha^{\text{NCF}}$ (mb)	$\sum \sigma_{tr}^{\text{PLF}}$ (mb)	σ_n^{tot} (mb)	$\sigma_n^{d-\text{exp}}$ (mb)	$\sigma_n^{c-\text{exp}}$ (mb)	$\sigma_n^{d-\text{Cal.}}$ (mb)	$\sigma_n^{c-\text{Cal.}}$ (mb)
^{12}C	1505 ± 46	226 ± 25	40 ± 7					
^{13}C	1515 ± 107	187 ± 40	30 ± 8	108 ± 10	86 ± 12	37 ± 8	68	30

the peak of the angular distribution around the grazing angle. The energy spectra of the ^{12}C band up to neutron binding energy (7.23 MeV) was assumed to be contributed by transfer to discrete states and it was considered as transfer to continuum above this energy. The area under the total, discrete, and continuum curves were estimated and the cross sections are given in Table II. The total transfer cross section turns out to be 108 ± 10 mb in which transfer to discrete states contributes to $\approx 80\%$ (86 mb) and transfer to continuum measured from ^{12}C band in PLF spectra were estimated to be 20% (22 mb).

The ^{12}C fragment after $1n$ transfer to continuum may also break resulting in α production. This part was not included in the measured one neutron transfer cross section as it was extracted using the ^{12}C band in the spectra of the (^{13}C , ^{12}C) reaction. The α particles from break up following neutron transfer to continuum was $\approx 24\%$ as estimated earlier which is equivalent to ≈ 15 mb assuming a α multiplicity of three. Thus the total transfer to continuum cross section is estimated to be $22 + 15 = 37$ mb as given in Table II.

V. $1n$ -TRANSFER TO CONTINUUM AND CONTINUUM DISCRETIZED COUPLED CHANNEL CALCULATIONS

The calculations have been performed with the CCBA method using the code FRESKO [40] to estimate the $1n$ transfer to discrete and continuum states. The spectroscopic factors were taken from the $^{93}\text{Nb}(d, p)$ reaction up to 2.32 MeV [41]. Ten more energy states were included from the ENSDF database and the spectroscopic factors for these states from 2.32 MeV to 6.5 MeV were assumed as an average of the last ten states below 2.32 MeV. Some unaccounted cross section might still be there as not all states were included below a neutron binding energy of 7.23 MeV. The excited states (4.44 MeV and 7.65 MeV) of ^{12}C were also coupled. In addition to discrete states, calculations were performed for continuum states up to 15 MeV above the neutron binding energy. The continuum energy states were distributed in equal momentum bins of width $\Delta k = 0.1 \text{ fm}^{-1}$. In Table II, a list of the experimental and the calculated values of $1n$ -transfer cross sections are given. The calculated integral values of both

discrete and continuum transfer cross sections are consistent with the experimental data. Similar to $1n$ transfer followed by the breakup of ^{12}C , a contribution from breakup of $^{8,9}\text{Be}$ following $^{5,4}\text{He}$ transfer is expected to be $< 2-3$ mb.

The breakup cross section was calculated using FRESKO with the CDCC method. The continuum above $^{13}\text{C} \rightarrow ^{12}\text{C} + 1n$ breakup threshold of 4.95 MeV was discretized into momentum bins of width $\Delta k = 0.3 \text{ fm}^{-1}$ up to ≈ 15 MeV with relative angular momentum $L = 0-5\hbar$. The input potentials for $^{12}\text{C} + ^{93}\text{Nb}$ were taken from Ref. [28] and for $n + ^{93}\text{Nb}$ it was obtained from Ref. [42]. The $^{13}\text{C} \rightarrow ^{12}\text{C} + 1n$ breakup cross section using CDCC calculations was obtained as 15 mb. This value obtained for elastic breakup is much smaller than the one neutron transfer cross section value of 108 mb.

VI. SUMMARY

In summary, measurement of α -particle spectra in $^{12,13}\text{C}$ induced reactions on ^{93}Nb at a bombarding energy of 65 MeV has been reported. From a detailed analysis of the spectra, contributions from direct break up and transfer processes, leading to the production of α particles were determined. A significant contribution of α particles resulting from the process like neutron transfer followed by the break up of ^{12}C in the case of ^{13}C projectile is observed. This is an interesting result being reported for strongly bound projectiles. The exclusive particle- γ measurements are required for various targets to further strengthen these findings.

ACKNOWLEDGMENTS

Two of us (S.K. and V.V.P.) acknowledge Indian National Science Academy for the support through the fellowship. Authors are thankful to the Mumbai Pelletron-Linac staff for the smooth running of the accelerator during the experiment. We thanks Drs. B.S. Tomar and A. Shrivastava for their helpful comments on this work. Thanks are also due to anonymous referee for the critical comments to improve the quality of the work.

- [1] P. Hodgson, *Nature (London)* **257**, 446 (1975).
 [2] M. Freer, H. Horiuchi, Y. Kanada-En'yo, D. Lee, and Ulf-G. Meißner, *Rev. Mod. Phys.* **90**, 035004 (2018).
 [3] Y. T. Oganessian, V. I. Zagrebaev, and J. S. Vaagen, *Phys. Rev. Lett.* **82**, 4996 (1999).

- [4] D. Singh, S. B. Linda, P. K. Giri, A. Mahato, R. Tripathi, H. Kumar, M. A. Ansari, N. P. M. Sathik, R. Ali, R. Kumar, S. Muralithar, and R. P. Singh, *Phys. Rev. C* **97**, 064604 (2018).
 [5] M. S. Zisman, F. D. Becchetti, B. G. Harvey, D. G. Kovar, J. Mahoney, and J. D. Sherman, *Phys. Rev. C* **8**, 1866 (1973).

- [6] D. R. Zolnowski, H. Yamada, S. E. Cala, A. C. Kahler, and T. T. Sugihara, *Phys. Rev. Lett.* **41**, 92 (1978).
- [7] R. deSouza, V. Singh, S. Hudan, Z. Lin, and C. Horowitz, *Phys. Lett. B* **814**, 136115 (2021).
- [8] J. Hong, G. Adamian, and N. Antonenko, *Phys. Lett. B* **805**, 135438 (2020).
- [9] T. Inamura, M. Ishihara, T. Fukuda, T. Shimoda, and H. Hiruta, *Phys. Lett. B* **68**, 51 (1977).
- [10] C. V. Christov, *Z. Phys. A* **325**, 221 (1986).
- [11] D. J. Parker, J. J. Hogan, and J. Asher, *Phys. Rev. C* **35**, 161 (1987).
- [12] S. Wald, S. B. Gazes, C. R. Albiston, Y. Chan, B. G. Harvey, M. J. Murphy, I. Tserruya, R. G. Stokstad, P. J. Countryman, K. Van Bibber, and H. Homeyer, *Phys. Rev. C* **32**, 894 (1985).
- [13] K. S. Babu, R. Tripathi, K. Sudarshan, B. D. Shrivastava, A. Goswami, and B. S. Tomar, *J. Phys. G: Nucl. Part. Phys.* **29**, 1011 (2003).
- [14] K. S. Babu, R. Tripathi, K. Sudarshan, S. Sodaye, A. Goswami, B. Shrivastava, and B. Tomar, *Nucl. Phys. A* **739**, 229 (2004).
- [15] H. Kumar, S. A. Tali, M. A. Ansari, D. Singh, R. Ali, A. Ali, S. Parashari, P. K. Giri, S. B. Linda, R. Kumar, R. P. Singh, and S. Muralithar, *Phys. Rev. C* **99**, 034610 (2019).
- [16] H. Morgenstern, W. Bohne, W. Galster, K. Grabisch, and A. Kyanowski, *Phys. Rev. Lett.* **52**, 1104 (1984).
- [17] K. Siwek-Wilczyńska, E. H. du Marchie van Voorthuysen, J. van Popta, R. H. Siemssen, and J. Wilczyński, *Phys. Rev. Lett.* **42**, 1599 (1979).
- [18] V. Jha, V. V. Parkar, and S. Kailas, *Phys. Rep.* **845**, 1 (2020), and references therein.
- [19] G.-M. Jin, Y.-X. Xie, Y.-T. Zhu, W.-G. Shen, X.-J. Sun, J.-S. Guo, G.-X. Liu, J.-S. Yu, C.-C. Sun, and J. Garrett, *Nucl. Phys. A* **349**, 285 (1980).
- [20] H. C. Britt and A. R. Quinon, *Phys. Rev.* **124**, 877 (1961).
- [21] V. V. Parkar, V. Jha, and S. Kailas (2021), private communication.
- [22] B. Wang, Z. Ren, and D. Bai, *Phys. Lett. B* **793**, 110 (2019).
- [23] A. D'Onofrio, H. Dumont, M.-G. Laurent, B. Delaunay, F. Terrasi, and J. Delaunay, *Nucl. Phys. A* **378**, 111 (1982).
- [24] G. Fruet, S. Courtin, M. Heine, D. G. Jenkins, P. Adsley, A. Brown, R. Canavan, W. N. Catford, E. Charon, D. Curien, S. DellaNegra, J. Duprat, F. Hammache, J. Lesrel, G. Lotay, A. Meyer, D. Montanari, L. Morris, M. Moukaddam, J. Nippert, Z. Podolyak, P. H. Regan, I. Ribaud, M. Richer, M. Rudigier, R. Shearman, N. deSereville, and C. Stodel, *Phys. Rev. Lett.* **124**, 192701 (2020).
- [25] J. J. Kolata, *Phys. Rev. C* **63**, 061604(R) (2001).
- [26] V. V. Parkar, V. Jha, and S. Kailas (2020), [arXiv:2001.02448](https://arxiv.org/abs/2001.02448).
- [27] H. Dumont, B. Delaunay, J. Delaunay, and D. M. D. C. Rizzo, *Nucl. Phys. A* **435**, 301 (1985).
- [28] T. N. Nag, R. Tripathi, S. Sodaye, K. Sudarshan, S. Santra, K. Ramachandran, A. Kundu, D. Chattopadhyay, A. Pal, and P. K. Pujari, *Phys. Rev. C* **102**, 024610 (2020).
- [29] W. von Oertzen and A. Vitturi, *Rep. Prog. Phys.* **64**, 1247 (2001).
- [30] E. F. Aguilera, J. J. Kolata, F. M. Nunes, F. D. Becchetti, P. A. DeYoung, M. Goupell, V. Guimaraes, B. Hughey, M. Y. Lee, D. Lizcano, E. Martinez-Quiroz, A. Nowlin, T. W. O'Donnell, G. F. Peaslee, D. Peterson, P. Santi, and R. White-Stevens, *Phys. Rev. Lett.* **84**, 5058 (2000).
- [31] R. Künkel *et al.*, *Z. Phys. A* **336**, 71 (1990).
- [32] H. Kumawat, V. Jha, V.V. Parkar, B. J. Roy, S. Santra, V. Kumar, D. Dutta, P. Shukla, L. M. Pant, A. K. Mohanty, R. K. Choudhury, and S. Kailas, *Phys. Rev. C* **81**, 054601 (2010).
- [33] A. Gavron, *Phys. Rev. C* **21**, 230 (1980).
- [34] D. J. Parker, J. Asher, T. W. Conlon, and I. Naqib, *Phys. Rev. C* **30**, 143 (1984).
- [35] Y. K. Gupta, B. John, D. C. Biswas, B. K. Nayak, A. Saxena, and R. K. Choudhury, *Phys. Rev. C* **78**, 054609 (2008).
- [36] J. Schiffer, H. Körner, R. Siemssen, K. Jones, and A. Schwarzschild, *Phys. Lett. B* **44**, 47 (1973).
- [37] M. Mermaz, R. Dayras, J. Barrette, B. Berthier, D. De Castro Rizzo, O. Cisse, R. Legrain, A. Pagano, E. Pollacco, H. Delagrangé *et al.*, *Nucl. Phys. A* **441**, 129 (1985).
- [38] W. Henning, Y. Eisen, H.-J. Körner, D. G. Kovar, J. P. Schiffer, S. Vigdor, and B. Zeidman, *Phys. Rev. C* **17**, 2245 (1978).
- [39] A. Winther, *Nucl. Phys. A* **572**, 191 (1994).
- [40] I. Thompson (2009), <https://github.com/I-Thompson/fresco>.
- [41] J. B. Moorhead and R. A. Moyer, *Phys. Rev.* **184**, 1205 (1969).
- [42] F. D. Becchetti and G. W. Greenlees, *Phys. Rev.* **182**, 1190 (1969).